Cryogenics 57 (2013) 140–149

Contents lists available at ScienceDirect

Cryogenics

journal homepage: www.elsevier.com/locate/cryogenics

Study of mixed refrigerant undergoing pulsating flow in micro coolers with pre-cooling

Ryan Lewis [a,*], Yunda Wang [a], Hayley Schneider [a], Y.C. Lee [a], Ray Radebaugh [b]

[a] University of Colorado at Boulder, Department of Mechanical Engineering, Boulder, CO, USA
[b] National Institute of Standards and Technology, Boulder, CO, USA[1]

ARTICLE INFO

Article history:
Received 4 January 2013
Received in revised form 25 June 2013
Accepted 1 July 2013
Available online 10 July 2013

Keywords:
Mixed refrigerant
Micro cooler
Two-phase flow
Pulsating flow

ABSTRACT

Micro cryogenic coolers can provide low temperatures with a smaller volumetric footprint and smaller power draw than their conventional-scale counterparts. However, they can exhibit lower-than-desired cooling power. We measure the specific cooling power of a refrigerant expanding from a high pressure of 0.6 MPa to a low pressure of 0.1 MPa, while undergoing pulsating flow in a micro cryogenic cooler with pre-cooling. We further observe that the pulses in the flow-rate occur due to a volume of liquid forming in the high-pressure coupling mini-channel. The composition of the flowing refrigerant is analyzed with gas chromatography and thermal conductivity detection (GC/TCD), showing that there is no overall composition change in the refrigerant after it enters the pre-cooling lines. A model of the cooling power under such a pulsating flow regime is developed with good agreement to measured values. An improved refrigerant mixture is designed with this model, and subsequently tested, showing increased specific cooling power.

1. Introduction

Micro low-temperature and cryogenic coolers are receiving increased attention in applications which benefit from low temperatures, but only require the dissipation of small heat loads. Such applications include infrared and terahertz detectors [1,2], low noise electronics [3], and high-temperature superconducting quantum interference devices [4]. Traditional miniature and micro-scale coolers include Stirling and Peltier coolers, but Joule–Thomson (J–T) based micro coolers are receiving considerable attention as well, because J–T coolers can be smaller than Stirling coolers and more efficient than Peltier coolers, when operating at temperatures below 200 K [5]. J–T micro cryogenic coolers (MCCs) can achieve their small size and high efficiency when using refrigerant mixtures.

Refrigerant mixtures can increase the specific cooling power compared to a pure refrigerant if the composition of the mixture is optimized. Operating with a well-designed refrigerant allows J–T coolers to reach cryogenic temperatures with typical working pressures of 2.0 MPa. Such refrigerant are non-azeotripic mixtures of hydrocarbons, hydrofluorocarbons, nobel gasses, and nitrogen [6]. However, the composition of the mixture can change due to preferential leaks or preferential dissolution in compressor lubricants. A leak-free and oil free system will eliminate those problems, but because the mixtures are non-azeotropic liquid hold-up in the channels will also change the overall composition [7]. For macro-scale (10 W capacity) J–T cooler systems, Narasimhan and Venkatarathnam have developed a method to compensate for this type of composition shift [8].

When coupling a J–T micro cooler to a mini or micro-scale compressor, the maximum discharge pressure of the compressor is limited to well below 2.0 MPa. Our group has shown that a J–T micro cooler can achieve temperatures of 200 K when connected to a compressor with a discharge pressure of 0.6 MPa and suction pressure of 0.1 MPa, when the cooler is pre-cooled to 273 K [9]. In such low-pressure operation the flow-rate of the system will either experience steady flow or pulsating flow. In both cases, the cooling power of the refrigerant has been measured to be lower than calculated. For steady flow, it has been shown that the refrigerant mixture composition will change due to hold-up of the liquid components in the macro-scale pre-cooled channels [10]. However, pulsating flow is less well understood.

It should be noted that this pulsating flow regime is different from other sources of cooling instability reported for J–T micro coolers. Previous MCC reports show that instability can be a result of clogging in the Joule–Thomson valve due to solid formation [11,12]. In macro-scale J–T coolers, ice can form clogs from trace moisture contaminants; a maximum of 2 parts per million (ppm) of water contaminant is recommended as a critical upper concentration, based on practical experience [12]. However in MEMS-scale channels, such as those used by Lerou et al. [11], ice clogging

* Corresponding author. Tel.: +1 5094383587.
E-mail address: rjlewis@colorado.edu (R. Lewis).
[1] Partial contribution of NIST, not subject to U.S. copyright.

0011-2275/$ - see front matter © 2013 Elsevier Ltd. All rights reserved.
http://dx.doi.org/10.1016/j.cryogenics.2013.07.001

will occur when water concentration is high enough that the partial pressure of water is above the sublimation/deposition point at that temperature. In reference [11], contaminant concentrations of roughly 0.1 ppm in nitrogen at 8 MPa led to ice formation at 200 K. In the present work, ice clogging is not the cause of pulsation, as is evident by the existence of pulsating flow at temperatures above 273 K. Another often cited cause of instability occurs due to a surplus of cooling power, which can lead to excess amounts of liquid forming downstream of the J–T valve [13], which leads to unsteady liquid flow in the low-pressure channels, and associated high-frequency low-amplitude temperature oscillations. This sort of flow was observed in microchannels by Burger et al. with liquid ethylene in his coaxial heat exchanger [14]. The pulsating flow experienced by the MCC under investigation is different as it corresponds to intermittent liquid flow across the J–T valve, as reported previously [10], rather than down-stream of the J–T valve.

This paper explores the pulsating flow regime of micro coolers by performing a visualization analysis study of refrigerant vapor/liquid 2-phase flow in the heat exchanger of the micro cooler, by measuring the isothermal enthalpy change of the refrigerant at different temperatures, and by measuring the composition of the refrigerant. Based on this analysis, a model of pulsating flow is presented that considers each pulse to be a slug of liquid that forms in the large pre-cooling channels and fills the micro-channels of the micro-cooler. This slug-based separation is new to the field of cryogenics. Such slug-based separation leads to a new method to calculate the specific cooling power of a refrigerant mixture, and this new calculation method is verified by designing and testing a modified refrigerant mixture with an increased cooling power.

2. Materials and methods

The micro cryogenic cooler (MCC) used in this experiment was designed by Lin et al. [15]. It operates under the Joule–Thomson cycle whereby compressed refrigerant enters the high pressure channels of a counter-flow heat exchanger (CFHX), expands to low pressure across a restriction (referred to as the "J–T valve") thereby cooling, and the cooled refrigerant returns though the low-pressure channels of the CFHX before returning to the suction port of the compressor. The MCC used for these tests uses 6 hollow-core glass fibers (ID/OD = 75/125 μm) as the high-pressure channel of the CFHX. The fibers are held in a capillary (ID/OD = 536/617 μm), and the interstitial space between the fibers within the capillary forms the low-pressure channel of the CFHX. The J–T valve is formed by anodic-bonding an etched silicon chip to a borosilicate glass chip. A gap etched into the silicon, measuring 1.5 μm in height provides the flow restriction. This MCC is shown in Fig. 1. Details on the fabrication and assembly of this device are described in [16]. Typically, the outer diameter of the capillary is coated in gold to decrease radiative heat loads. However, in order to facilitate the visualization experiment, a MCC without the gold coating was assembled, as shown in Fig. 1c. The warm end of the CFHX is connected to a macro-coupler, which is fastened to a base-plate flange, as in Fig. 1d. The base-plate flange allows the MCC to be placed in a vacuum using standard vacuum fittings.

The compressor used in these experiments was formed from a commercial piston-oscillator coupled to custom micro-fabricated check valves. More information on the compressor can be found in [9]. The experimental set-up is shown in Fig. 2. The suction and discharge pressures of the compressor are monitored with pressure transducers. After the refrigerant is compressed, it passes through 1 g of 0.3 nm molecular sieve to remove any trace water contaminants. It also passes across a 7 μm particulates filter. The pressure after the filter and sieve is monitored. The refrigerant then travels through roughly 10 cm of copper tubing (ID/OD = 1.4/3.2 mm), before reaching the MCC. Downstream of the MCC, the flow-rate of the refrigerant is measured with a mass flow-meter. The MCC is held under a vacuum of 1–10 Pa (10^{-5}–10^{-4} Torr), which ensures that any heat loads due to convection or conduction through the air are negligible.

Before running the compressor, all refrigeration lines are evacuated to 10 Pa (10^{-4} Torr). Mixed refrigerant regulated at 0.1 MPa

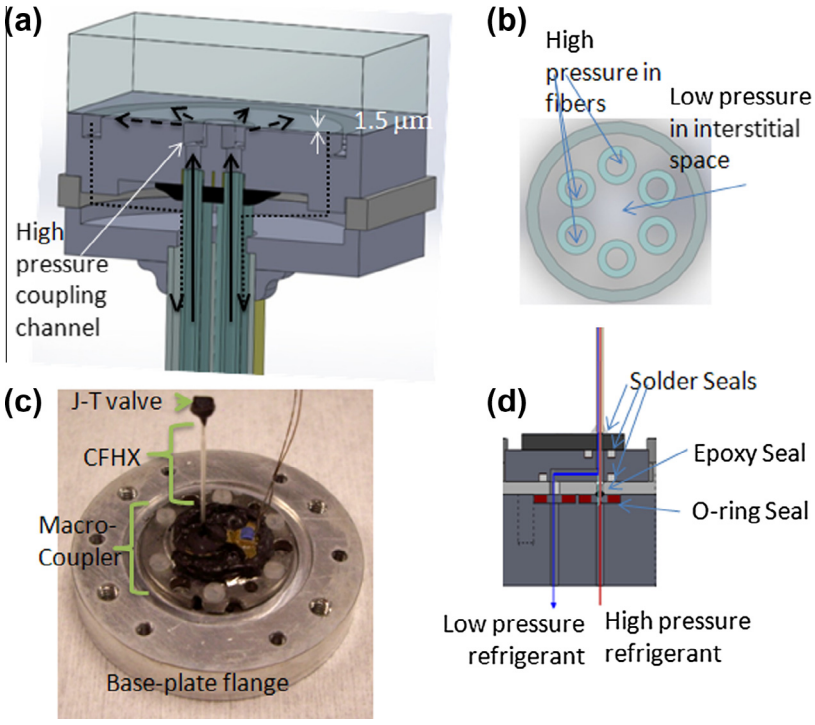

Fig. 1. The MCC used in these tests. (a) cross-sectional drawing of the J–T valve, showing path of the refrigerant as it expands from high pressure (solid line) to low pressure (dotted line), (b) cross-section of the CFHX, (c) photograph of a MCC assembled without gold coating, and (d) drawing showing assembly of the MCC to the base-plate flange.

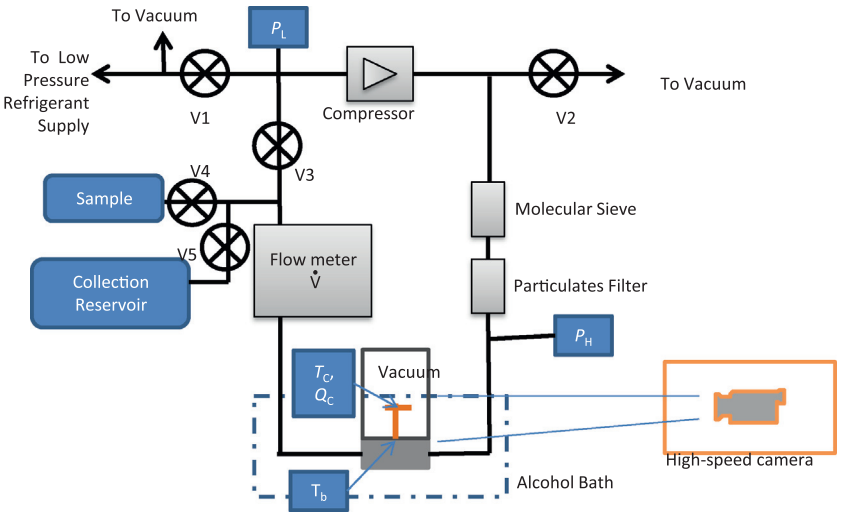

Fig. 2. Schematic of the test set-up. Measured data include: high pressure (P_H), low pressure (P_L), flow-rate ($\dot{V}$), MCC base temperature (T_B), MCC cold-end temperature (T_c), and heat into the MCC cold-end (Q_c).

is fed to the suction port of the compressor and allowed to pass through the compressor check valves such that the system starts with an internal pressure of 0.1 MPa. When the compressor is turned on, the high-pressure takes a period of time to develop. During this initial starting period, the system experiences steady flow-rates. If no pre-cooling were applied, the steady flow regime would persist. However, if pre-cooling is applied to the MCC base-plate flange, then after a period of time the flow will transition to a pulsating regime [9].

For the visualization study, only the base-plate flange is pre-cooled. A high-speed visual camera with frame-rates up to 10,000 fps is connected to an optical microscope, and captures the movement of liquid in the fibers of the heat exchanger and in the J–T valve gap. It was found that operation at frame rates higher than 3000 fps required illumination that posed an unacceptable heat load to the MCC.

The composition of the refrigerant was measured with gas chromatography and thermal conductivity detection (GC/TCD) at a commercial natural gas analysis lab. Samples of refrigerant were taken by closing Valve 3 (shown in Fig. 2), and slowly opening the valve to an evacuated bottle. During the initial start-up period of the test, refrigerant was collected in a low-pressure reservoir by opening Valve 5. Once pulsations developed and continued for 10 min, the refrigerant was collected into the sample bottle by closing Valve 5 and opening Valve 4. Three samples were collected in this manner: one with 255 K pre-cooling and pulsations, another with 275 K pre-cooling and pulsations, and one with neither pre-cooling nor pulsations at 295 K.

To measure the isothermal enthalpy change of the refrigerant, the method described in [10] is applied, and briefly repeated here. The MCC is shrouded in a radiation shield, and a platinum resistance thermometer (PRT) is mounted onto the J–T valve. The vacuum package and 10 cm of coupling line is held in an alcohol bath to pre-cool the MCC macro-coupler and incoming refrigerant. The temperature at the J–T valve, macro-coupler, and radiation shield are all monitored. A small voltage is applied to the PRT at the J–T valve, causing it to heat up. The voltage is controlled such that the temperature of the J–T valve is increased to that of the macro-coupler. That required heat input gives the net heat load to the MCC. Adding net heat to parasitic loads due to radiation and conduction gives the gross cooling power. Dividing the gross cooling power by the molar flow-rate yields the specific isothermal enthalpy difference of the mixture at the J–T valve temperature.

Table 1
The compositions of the 3 mixtures studied for isothermal enthalpy difference tests.

200 K Mix	140 K Mix	160 K Mix
8% Methane	34% Methane	24% Methane
46% Ethane	20% Ethane	36% Ethylene
14% Propane	18% Ethylene	14% Propane
4% Butane	16% Isobutane	10% Isopentane
28% Pentane	12% Isohexane	16% Pentane

Each isothermal enthalpy measurement is taken at a single alcohol bath temperature, and measures the applied heat over at least 6 pulsation cycles, which takes 5–10 min. Afterward, the alcohol bath temperature is changed, and the next data point is measured.

Three refrigerant mixtures were studied in this test. They were designed to cool from 300 K on the warm-end to 200 K, 160 K, and 140 K. These mixtures are referred to as the "200 K Mix," "160 K Mix," and "140 K Mix," respectively. Their compositions are listed in Table 1. The gross cooling power of a Joule-Thomson cooler is given by the product of the flow-rate ($\dot{n}$) with the minimum isothermal enthalpy difference between the high-pressure stream and low-pressure stream, minimized across the temperature range experience by the heat exchanger: $(\Delta h|_T)_{min}$ [17]. The composition of the 3 mixtures was chosen to maximize $(\Delta h|_T)_{min}$ between a high pressure of 0.4 MPa and a low pressure of 0.1 MPa, over the listed temperature range. The high pressure of 0.4 MPa was selected to allow these refrigerant mixtures to be used with generic low-pressure micro compressors. In the present work, our compressor generates higher pressures. The program NIST4, which uses thermophysical properties calculated with the NIST software SUPERTRAPP was used to perform the optimization [18]. The $\Delta h|_T$ curves for each mixture are plotted in Fig. 3. At the high pressure but at ambient temperature (i.e. in the conditions experienced between the compressor discharge and the pre-cooling lines), some fraction of each refrigerant will liquefy, and the compositions of the liquid and vapor can be calculated from an equation of state.

3. Results

3.1. Two-phase flow visualization

The visualization tests are performed with the 200 K Mix. During the visualization tests, radiative heat loads prevented the MCC cold-end from cooling below 278 K during steady flow, even with

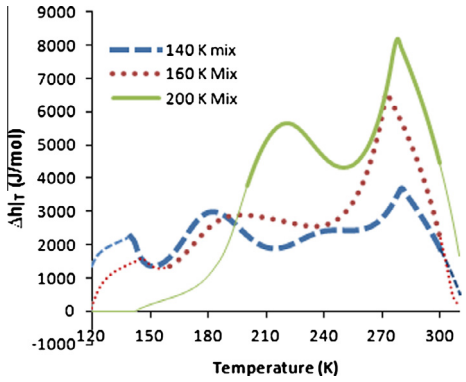

Fig. 3. Isothermal enthalpy difference curves of the 3 mixtures used in the enthalpy measurement test, calculated between a pressure of 0.4 and 0.1 MPa, using the software REFPROP [19]. The regions where the refrigerant was designed to operate are shown in bold in the figure.

the MCC base cooled to 273 K. During steady flow, no liquid is observed in the fibers. After nearly two hours the first pulse in flow-rate occurs. Each pulse in flow-rate is accompanied by an increase in cooling performance, as shown in Fig. 4, with an overall minimum temperature of 243 K.

The observed flow patterns in the fibers are as follows: first, the fiber is in single-phase vapor flow. Then abruptly a front of liquid passes into the fiber from the macro-coupler and fills the fiber with liquid. This corresponds to the pulse in the flow-rate. The fiber experiences single-phase liquid flow for a short period of time, after which there is a transitional period that contains 2-phase flow, in the form of vapor bubbles, small slugs of liquid, or liquid slug-annular rings. After a period of this 2-phase flow, the fiber dries out and experiences single-phase vapor flow again, and the cycle repeats. Such flow-patterns are shown in Fig. 5.

The speed of the liquid front as it passes through the fibers was determined from the video data to be 7.44 mm/s on average, which agrees well with a speed calculated from the ratio of molar flow-rate with density-times-area: $v = \dot{n}/\rho A$. Here density is calculated for the liquid components of the mixture at 273 K and 0.54 MPa.

Once a liquid pulse reaches the J–T valve, it quickly crosses the radial gap. But in the high-pressure coupling channel of the J–T valve chip, 0.14 μL of vapor will have to drain across the gap at the same time the liquid is flowing. As a result, liquid will not fully fill the J–T valve gap even if the fibers are experiencing single-phase liquid flow, as shown in Fig. 6a–c. After the liquid pulse passes through the J–T valve, some of the low-pressure channel

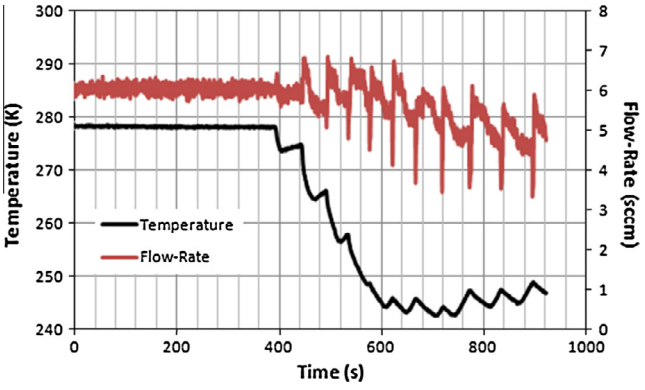

Fig. 4. Temperature curve (black) and flow-rate curve (red online, grey in print) of the MCC as it experiences its first pulses during visualization studies. Note that each pulse in flow-rate brings about greater cooling.

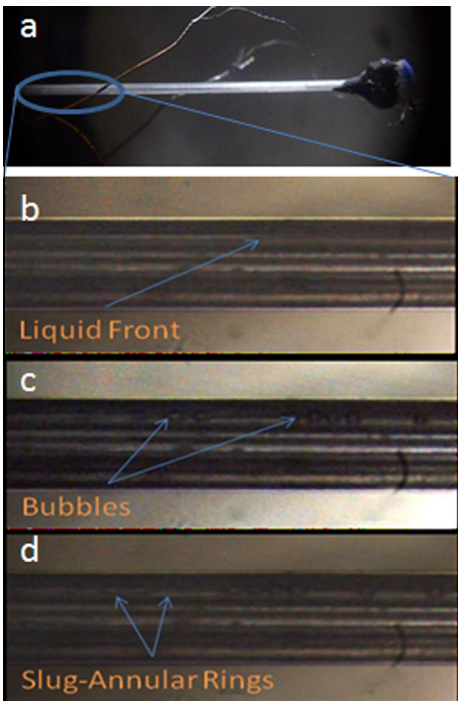

Fig. 5. Flow patterns observed in the fibers of the micro-cooler during pulsating flow. (a) zoomed out photo of MCC to illustrate what portion of the CFHX is shown in the microscope images, (b) liquid front in the fiber traversing from warm inlet (left side) to cold-end (note that the region to the right of the arrow appears darker), (c) bubbles in the fiber, and (d) slug-annular rings during the transition from liquid flow to vapor flow.

will fill with liquid, shown in Fig. 6e and f. The low-pressure liquid can travel half of the way down the CFHX, but once the fibers contain 2-phase transitional flow, the liquid front in the low-pressure channel will retreat back to the J–T valve, and will dry out. When liquid from the 2-phase transitional flow reaches the J–T valve, it crosses the gap in the form of an "exploding film" as shown in Fig. 6d.

The transitions between each of the flow regimes all appear in the temperature and flow-rate profiles, shown in Fig. 7. Liquid-phase refrigerants tend to have the highest cooling power owing to the fact that they can evaporate and the heat absorbed in order to facilitate phase change is large. During the single-phase liquid flow, the cooling power is the highest, and the temperature of the MCC cold-tip drops. During the 2-phase transitional flows, the cooling power will slowly drop as less liquid flows, and the temperature will stop dropping and start to rise. During vapor flow, the cooling power of the refrigerant is quite low, so the temperature will rise. The transition from vapor flow to liquid flow is abrupt, and results in an abrupt change from rising temperature to falling temperature.

3.2. Isothermal enthalpy difference measurement

The results of the isothermal enthalpy test are shown in Fig. 8. To measure the isothermal enthalpy difference of the 200 K Mix, the alcohol bath started at 280 K and the flow was steady. The bath was cooled down to 253 K over 1 h, by which time pulses developed. After collecting data for 8 min at 250 K, the alcohol bath was then warmed in increments of roughly 5 K, while a $\Delta h|_T$ data point was measured at each temperature point ("Up 1" in Fig. 9a). After the bath temperature reached 280 K, the bath temperature was dropped again in increments of ~5 K, and enthalpy points were measured, to ensure that hysteresis was not affecting the

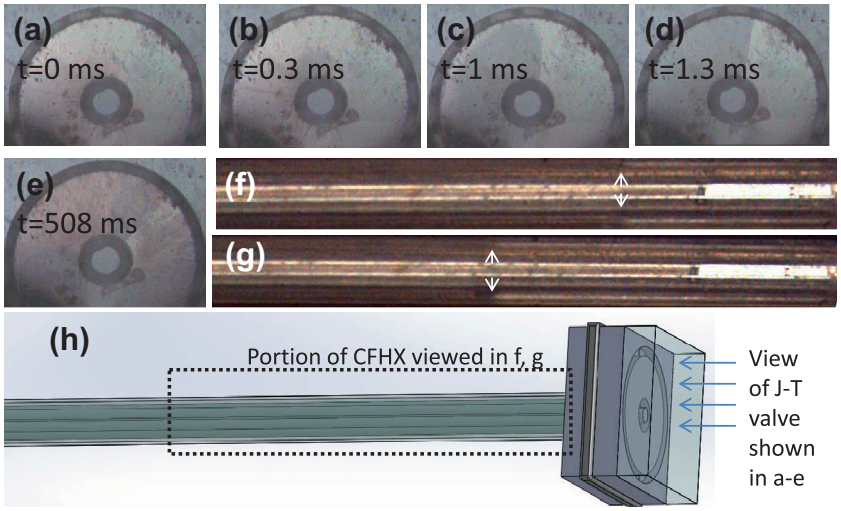

Fig. 6. Liquid as it passes through the J–T valve and low-pressure channel. (a–d) a liquid pulse crossing the J–T valve over 1.3 ms. The liquid is the darker portion in the radial expansion area. Note that even when the liquid has fully crossed the J–T valve, some vapor will still flow. (e) "Exploding film" as the flow transitions from vapor to 2-phase. (f and g) Liquid front advancing down the low-pressure channel of the CFHX. Liquid front location is shown with arrows. (h) A schematic showing which region of the CFHX and J–T valve is shown.

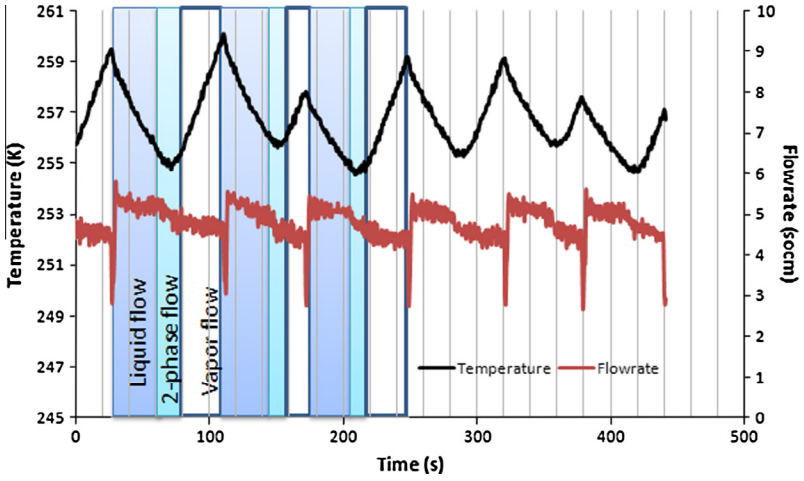

Fig. 7. Temperature and flow-rate curves with liquid/vapor flow regime pointed out.

measured enthalpy data ("Down 1"). Finally, a second set of enthalpy data were measured while the temperature was increased in increments to 286 K ("Up 2"). During this data run, the typical high-side pressure was 0.594 MPa. Additionally, several weeks later the system was evacuated and re-charged with refrigerant, and the test repeated ("Up 3"). The enthalpy data are plotted in Fig. 8. As in [10], the error bars on each point are taken as the standard deviation in $\Delta h|_T$ between each pulsation cycle. Also included in Fig. 8 is the enthalpy change calculated by REFPROP [19] for the original 200 K mixture (dotted line).

Previous studies have shown that liquid hold-up will change the mixture before it reaches the pre-cooled lines, and that in this experimental set-up that the refrigerant will effectively experience 100% liquid hold-up in the room-temperature lines [10]. The composition of the refrigerant entering the pre-cooled lines can therefore be calculated by finding the composition of the vapor. At 295 K and 0.594 MPa, REFPROP gives a composition of 11.4% methane, 61.1% ethane, 15.9% propane, 2.7% butane, and 8.8% pentane, by molar fraction. The enthalpy difference of this mixture resulting from liquid hold-up at 295 K and 0.594 MPa is plotted in Fig. 8 as well (dashed line). The solid lines are calculated according to a method presented in Section 4.3. For the 200 K mixture, the measured enthalpy data during pulsating flow are more than one standard deviation lower than those calculated with the mixture after experiencing room-temperature liquid hold-up (dashed line), but agree well with the calculation of pulsating flow presented in Section 4.3.

The isothermal enthalpy difference was also measured for the 160 K mix and 140 K mix, in Fig. 8b and c. Note for these two mixtures, the measured enthalpy difference is considerably lower than that calculated for either the original mixtures or the mixtures after room-temperature liquid hold-up.

3.3. Non-isothermal cooling power

During normal operation of the micro cryogenic cooler, there is a large temperature gradient across the heat exchanger. For a cooler experiencing a steady flow, the specific cooling power is given by the minimum in isothermal enthalpy difference within the temperature range experienced by the heat exchanger: $\dot{Q}/\dot{n} = (\Delta h|_T)_{min}$. With refrigerant experiencing pulsating flow, however, the cooling power may be different than this expression,

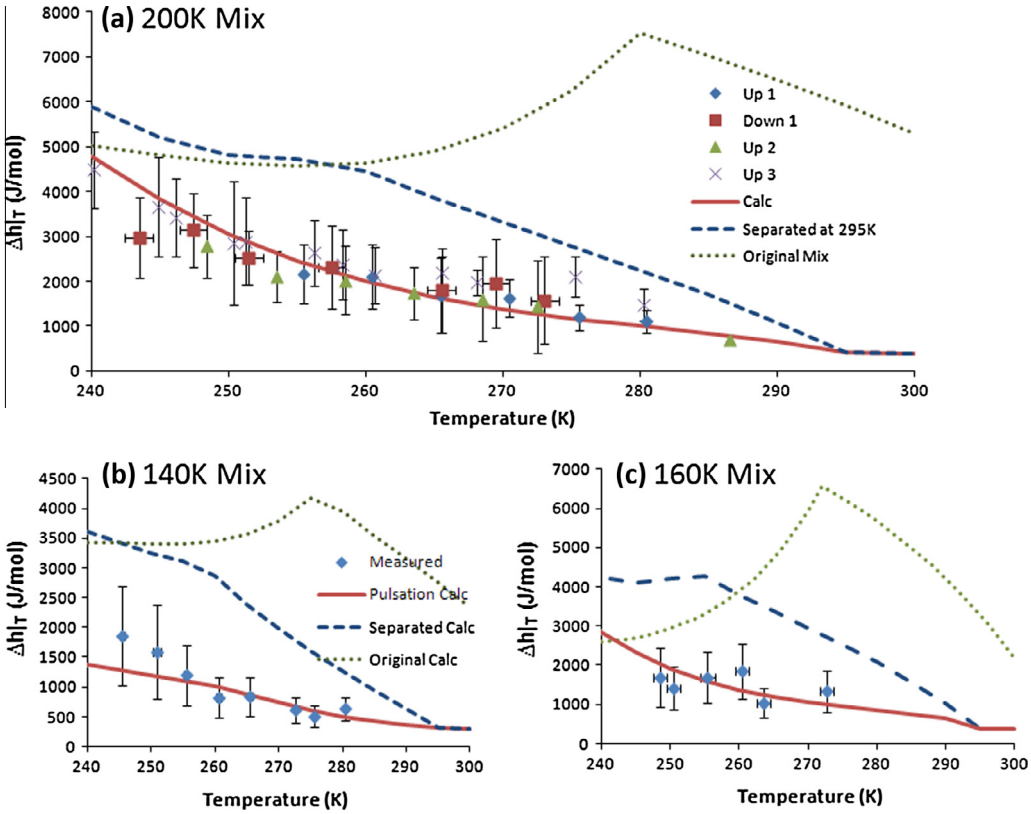

Fig. 8. Measured and calculated isothermal enthalpy differences of (a) 200 K Mix, (b) 140 K Mix, and (c) 160 K Mix. The dotted lines are calculations based on the original mixture, the dashed lines are calculations of the enthalpy difference after the liquid components of the mixture have been removed due to room-temperature liquid holdup, and the solid lines are calculations based on pulsing, as presented in Section 4.3.

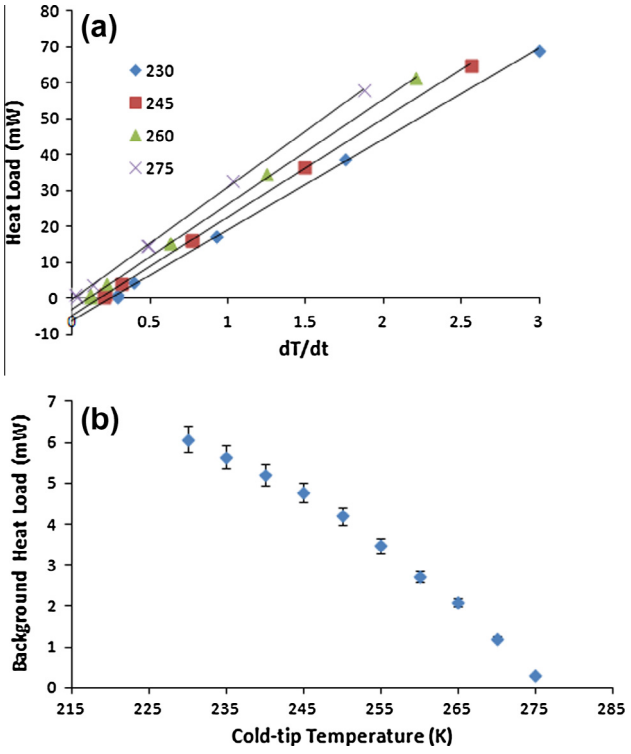

Fig. 9. (a) The heat loads plotted against rate of temperature rise 4 different temperatures, (b) measured parasitic heat loads as a function of cold-tip temperature.

and needs to be measured. The gross cooling power will be given by the sum of the applied cooling power (as in the previous section), and the parasitic heat loads. In this experiment, a second MCC was used which has a gold-coated heat exchanger. Two measurements of applied cooling power at various cold-tip temperatures were performed to demonstrate repeatability.

To determine the parasitic heat loads, a background heat leak test was performed on the MCC with ice pre-cooling, as described in [20]. The heat leak test proceeds as follows: first the MCC cools to 195 K with the 200 K Mix and ice pre-cooling. Second, a constant amount of heat is applied to the PRT. Simultaneously, the compressor is turned off and the high-side pressure is vented, such that the flow-rate through the MCC drops to zero and there is no active cooling. This will cause the temperature of the MCC to rise. Third, steps 1 and 2 are repeated with a different amount of heat applied to the PRT. The temperature rise rates are plotted against applied heat, at various temperatures, in Fig. 9a. Note that for each temperature, the rise rate is linear with applied heat. Extrapolating to a rise rate of 0, one finds a negative heat. This is the heat dissipated by the cooler in order for it to maintain that temperature—that is to say the parasitic heat load. The parasitic loads are plotted against temperature in Fig. 9b. Data with temperatures below 230 K are influenced by transient heating effects, and do not accurately reflect the parasitic heat load, so they are not included.

Knowing the parasitic heat loads, the applied cooling power is found by cooling the MCC to 200 K and stepping up the temperature by adjusting the applied heat load, as in Fig. 10a. The warm-end temperature for this measurement was kept at 273 K with the ice-bath. Finally, the specific cooling power is found by dividing the gross cooling power (sum of applied heat load and background heat load) by the flow-rate. The measured specific cooling power is

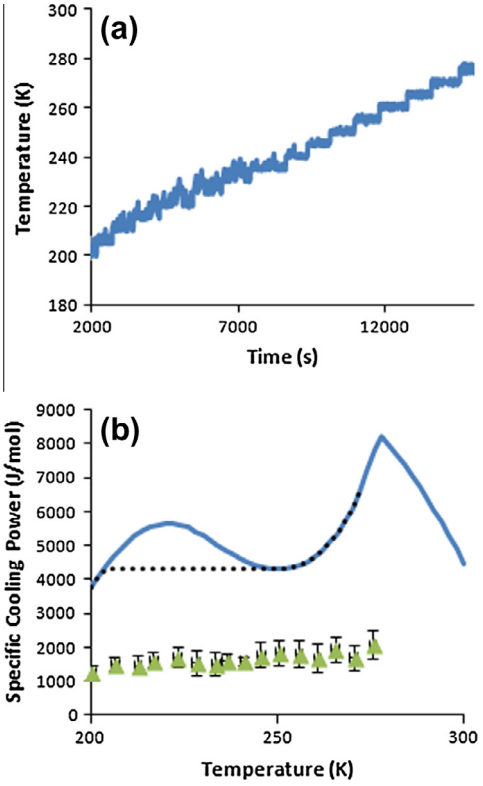

Fig. 10. (a) Temperature profile as heat was added to increase the temperature in steps and measure the cooling power, (b) measured (triangles) and calculated (dotted line) specific cooling powers of the 200 K Mix with pre-cooling to 273 K, as a function of cold-tip temperature. Calculations are performed according to $\dot{Q}/\dot{n} = (\Delta h|_T)_{min}$, minimized between the pre-cooling temperature (273 K) and the cold-tip temperature (variable). The solid line is $\Delta h|_T$ as a function of temperature, for reference.

plotted against cold-tip temperature in Fig. 10b. The solid line in Fig. 10b is the calculated isothermal enthalpy difference of the original mixture, and the dotted line is the $(\Delta h|_T)_{min}$ value of the original mixture with a warm-end temperature of 273 K, plotted against cold-end temperature.

3.4. Composition analysis

Once the test set-up was modified to collect refrigerant for analysis, two runs of pulsating refrigerant collection were performed. In the first, the refrigerant was pre-cooled to 251 K with a high-side pressure of 0.355 MPa, and in the second the refrigerant was pre-cooled to 273 K with a high-side pressure of 0.360 MPa. During the first run, exposure of the macro-coupler in the MCC to low temperatures over a long period of time caused a hairline fracture in one of the epoxy joints in the macro-coupler, which caused a small leak rate in the MCC, resulting in a vacuum pressure of 20 Pa, rather than 10 Pa as desired. The leak rate was more drastic during liquid flow, increasing the vacuum pressure as high as 100 Pa during a liquid pulse. This selective leak introduced some uncertainty between the measured composition and the composition flowing through the MCC. The measured composition therefore had less of the heavy components, which escaped through leakage. This uncertainty is captured with the error bars in Fig. 11.

A third collection run was performed without pre-cooling under steady flow-conditions at 295 K and 0.38 MPa on the high-side. The resulting concentrations are shown in Fig. 11. Note that the change in the concentrations at different levels of pre-cooling is within the experimental uncertainty of the measurement, and that

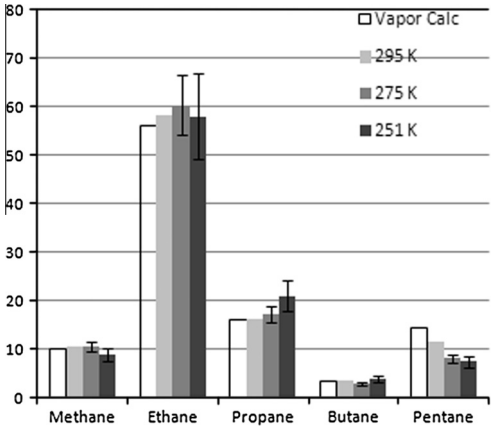

Fig. 11. Molar concentration of the 5 components in the 200 K Mix after running with pre-cooling at 3 different temperatures.

all concentrations agree reasonably well with composition of the vapor at 295 K and 0.38 MPa, which is calculated to be 10.0% methane, 56.0% ethane, 16.0% propane, 3.5% butane, and 14.5% pentane, and shown as the outlined bars in Fig. 11. This contrasts sharply with steady-flow in which the concentrations were a strong function of pre-cooling temperature, varying by up to 80% [10]. It appears that liquid is still held-up in the room-temperature coupling channels, but with pulsations liquid is no longer held in the pre-cooled channels.

4. Discussion

4.1. Pulses

According to the visualization data, pulses originate in the high pressure coupling lines, upstream of the MCC. According to the GC/TCD data, the bulk refrigerant during pulsating flow is the same as that which experiences complete liquid hold-up in the room temperature lines. These can be understood in terms of liquid slugs forming in the pre-cooled lines.

Consider a cool-down test of the 200 K Mix. Initially the original mixture fills all of the refrigerant lines, at a pressure of 0.1 MPa. Once the compressor starts running, the high-side pressure builds up, and once it is above 0.206 MPa (the 200 K Mix dew point at 295 K), liquid will start to form. The liquid will form along the walls in order to reduce surface energy. Due to a no-slip boundary condition along the walls, the liquid phase will move much slower than the vapor phase. For laminar annular flow, it has been shown that the liquid molar flux will be <0.01% of the vapor molar flux [10]. As the pressure continues to build to 0.6 MPa, more of the heavy components liquefy along the walls. Without pre-cooling, eventually all of the liquid components will be held along the walls, and only the vapor components will be in circulation. If the volumes of the high-pressure and low-pressure channels were equal and all of the liquid components present in the initial refrigerant charge were coated on the walls of the high-pressure channel, the molar liquid fraction in the high-pressure channel would be:

$$X_{l,h} = \frac{P_h/P_l + 1}{P_h/P_l + 1 + (P_h/P_l)(1 - X_l)X_l} \quad (1)$$

where $X_{l,h}$ is the molar liquid fraction in the high-pressure channel, P_h the pressure of the high-pressure channel (0.6 MPa), P_l the pressure of the low-pressure channel (0.1 MPa), and X_l the liquid fraction of the refrigerant resulting from a flash equilibrium at the high pressure and ambient temperature (0.311 as calculated by

REFPROP for the 200 K Mix). At a pressure ratio of 6:1, Eq. (1) yields 0.345. Note that $X_{l,h}$ will be larger than X_l because $X_{l,h}$ includes liquefied components that originated in both the high-pressure channels and low-pressure channels. Previous studies have shown that a critical liquid fraction of $X_{l,h} > 0.61$ is required for slugs to form [20].

However once the 295 K vapor reaches the pre-cooled lines, the temperature is below the dew point of the non-pre-cooled vapor components, so more liquid will form on the walls of the pre-cooled lines. As more of the refrigerant passes across the pre-cooled lines, the thickness of the liquid film will increase further. Eventually the thickness would reach a critical thickness, where surface tension in the radial direction overcomes inertia, viscosity, and surface tension in the axial direction, and the liquid film will form a slug of liquid. Such a slug will have a volume of roughly: $V = 2/3\pi r^3$ which for a channel radius of 1.3 mm gives a slug volume of 4.6 μL.

This is larger than the volume of the fibers in the MCC (0.57 μL), so the liquid can completely fill the fibers before any vapor enters the flow. The composition of the liquid will be given by the liquid components of the mixture, separated at the pre-cooling temperature. Once vapor enters the flow, the liquid that is already in the fibers take time to dry out, and the fiber experiences 2-phase flow. In this manner, eventually all of the modified refrigerant will pass through the MCC, just not all at once. First the liquefied components will pass, and then the vaporized components will pass.

4.2. Pulsation frequency

This model of pulses predicts that a pulse will occur whenever enough liquid forms upstream of the MCC to form a slug. The volume of the slug would be a function of geometry and thus constant over different mixtures. The frequency of pulsation would then be given by:

$$F = \frac{\dot{n} X_l}{V_{\rho l}}$$

Looking at the data from the isothermal enthalpy test, the frequency of pulsations is plotted against the liquid fraction of each mixture, shown in Fig. 12a. The liquid fraction is calculated by first removing the components due to liquid hold up at room temperature, and then calculating the molar liquid fraction of the remaining mixture at the pre-cooling temperature, and high-side pressure. The frequency is linear with molar liquid fraction, with different flow-rates having different slopes. In Fig. 12b, the ratio of frequency and flow-rate is plotted against liquid fraction, and all of the data fall on the same line. The inverse of the slope gives the slugs to be 70 μmol, or 6.4 μL with a density of 11 mol/L.

4.3. Isothermal enthalpy difference measurement

Such a flow regime would also change the isothermal enthalpy difference measured across a J–T valve. The overall cooling power of a single period of pulsation undergoing isothermal expansion is given by:

$$\dot{Q}_{gross} = \frac{1}{\tau_T}\left(\int_{\tau v} \dot{Q}_v dt + \int_{\tau l} \dot{Q}_l dt\right) = \frac{\tau_l}{\tau_T}\dot{n}_l \Delta h_l + \frac{\tau_v}{\tau_T}\dot{n}_v \Delta h_v \quad (2)$$

Here, τ_l τ_v and τ_T are the period of liquid flow, vapor flow, and total pulse period. The term Δh_l is the change in enthalpy of the components which are in liquid form in the high-pressure stream, as they expand from high pressure to low pressure. Because the term $\frac{\tau_l}{\tau_T}\dot{n}_l$ will give the total flow-rate times the liquid fraction, and similarly $\frac{\tau_v}{\tau_T}\dot{n}_v$ gives the total flow-rate times the vapor fraction, Eq. (2) gives a measured isothermal enthalpy difference of:

$$\frac{\dot{Q}}{\dot{n}} = X_l \Delta h_l + (1 - X_l)\Delta h_v \quad (3)$$

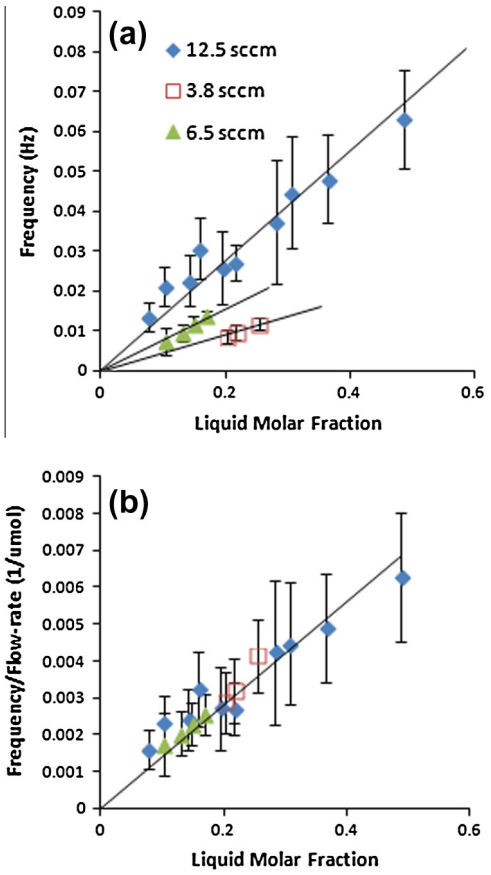

Fig. 12. (a) Frequency of pulses as a function of liquid molar fraction for 3 different flow-rates, and (b) the ratio of frequency and flow-rate as a function of liquid molar fraction. Note that the relative uncertainty is higher in 12b—this is due a higher flow-rate relative uncertainty of up to 20%, which reflects the uncertain nature of the flow-rate pulses.

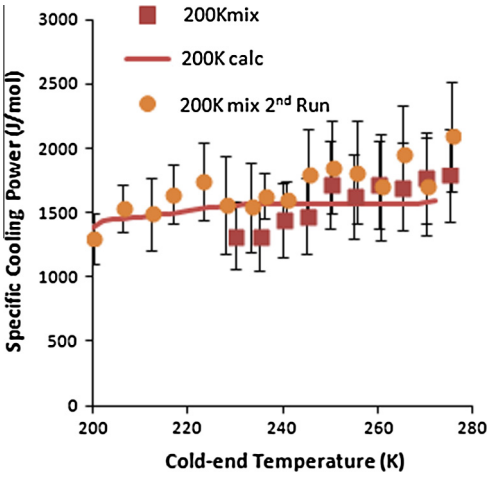

Fig. 13. Calculation of the specific cooling power of the 200 K Mix, plotted with measured values. The measurement was performed on 2 separate occasions, labeled "200 K Mix" and "200 K Mix 2nd Run", in order to demonstrate repeatability of the results.

The authors term this the "pulse averaged" enthalpy difference, and it is calculated for the 3 mixtures measured, and plotted against the measured isothermal enthalpy differences in Fig. 8, showing very good agreement. Such "pulse averaging" will necessarily result in a lower cooling power than that of the overall

Table 2
Composition of 2 mixtures modified by adding an isobutane/helium mix to the 200 K Mix.

	Mix A (%)	Mix B (%)
Methane	5.60	6.40
Ethane	32.20	36.80
Propane	9.80	11.20
Butane	2.80	3.20
Pentane	19.60	22.40
Iso-butane	26.70	17.80
Helium	3.30	2.20

mixture. This is because during the liquid pulse, some liquid will pass into the low-pressure side of the heat exchanger, and its evaporation will serve to cool the base of the MCC rather than the cold-end.

When the MCC experiences a temperature gradient, a similar analysis can be applied, by replacing the Δh terms with $(\Delta h|_T)_{\min}$ terms. The end result gives the specific cooling power of a mixture as:

$$\frac{\dot{Q}}{\dot{n}} = X_l(\Delta h_l|_T)_{min} + (1 - X_l)(\Delta h_v|_T)_{min} \quad (4)$$

This pulse averaged enthalpy difference is calculated for the 200 K Mix, shown in Fig. 13.

4.4. Modified mixture

Refrigerant mixtures for MCCs operating in the pulsating flow regimes can be designed to increase the pulse-averaged enthalpy difference. This is demonstrated by adding isobutane to the 200 K Mix. Two modified mixtures (Mix A and B) were mixed, with composition is listed in Table 2. Unfortunately the modification process introduced some helium contaminants, but Mix A and B still show enhanced performance. The isothermal enthalpy difference of these mixtures is measured and plotted in Fig. 14a. The specific cooling power in the range of 205–275 K of Mix A is measured with 273 K pre-cooling, and plotted in Fig. 14b. The solid lines in Fig. 14a and b are calculated values, using the above calculation method.

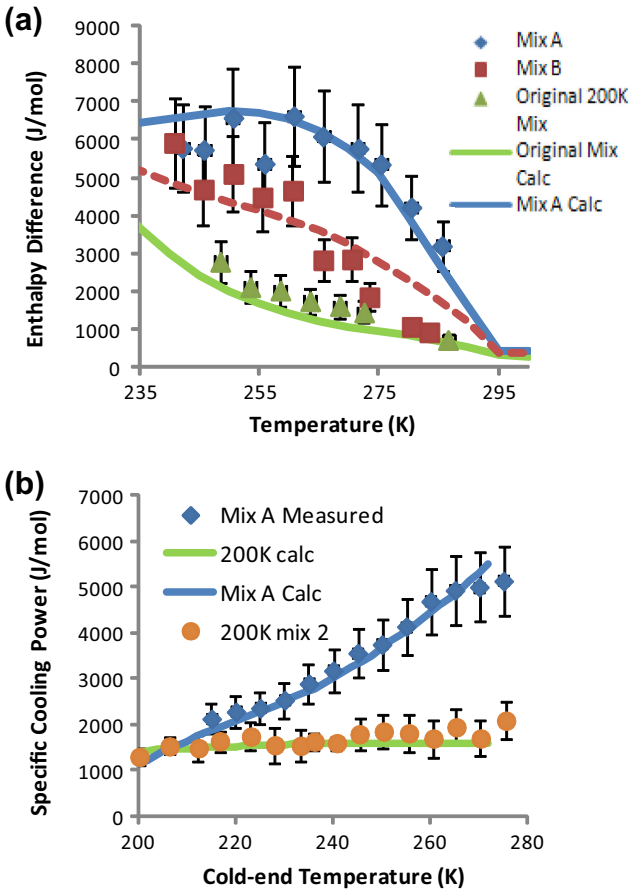

Fig. 14. Measured and calculated specific cooling powers of the original and modified 200 K Mix. (a) Isothermal enthalpy difference of Mix A, Mix B, and the original 200 K Mix. (b) Specific cooling power of Mix A and the original 200 K Mix as a function of cold-side temperature with the warm-end of the MCC pre-cooled to 273 K.

4.5. Pulsating flows in other MCCs

Pulsating flows of this nature will occur whenever non-azeotropic liquid slugs form in a mini-channel but are then transferred to a micro-channel heat exchanger. This will happen in any mixed refrigerant MCC that uses mini-scale coupling channels for pre-cooling. Such flow pulsations have been observed in a second MCC running mixed refrigerant, which used a polymer-based parallel-plate type heat exchanger. Pulses have also been observed in a larger scale steel-based MCC, which used a tube-in-tube heat exchanger [21]. It is apparent that the geometry of the heat exchanger is not a factor in forming flow pulses, as the pulses form in the coupling lines upstream of the heat exchanger.

Were one to eliminate the pre-cooling lines, and instead perform pre-cooling on the micro-channels directly, such large liquid pulses would be eliminated. Some of the cooling power lost due to the temporal separation of the refrigerant may be recovered. However, micro liquid slugs may still form, and may result in some different micro-pulse cooling power. Further studies are required of multi-phase microchannel flow on refrigerant mixtures undergoing phase change.

5. Conclusions

This article presents a study of mixed refrigerant in a micro cryogenic cooler undergoing a pulsating flow regime. The pulsating flow regime was visualized with high-speed video microscopy, the composition of the refrigerant mixture was measured with GC/TCD methods, and the isothermal enthalpy difference of multiple refrigerant mixtures was measured. The following conclusions can be drawn:

- Pulsating flows correspond to the buildup of a large slug of liquid upstream of the high pressure micro-channel CFHX. The slug of liquid has a larger volume than the CFHX high pressure channels, and fills them with liquid during a pulse. The MCC experiences all-vapor, all-liquid, and a brief 2-phase transitional flow.
- The overall composition of refrigerant passing through the MCC does not depend on the pre-cooling temperature, but the composition of the all-liquid and all-vapor phases of the refrigerant will depend on pre-cooling temperature.
- The average isothermal enthalpy difference of the refrigerant will be given by Eq. (3), and the specific cooling power will be given by Eq. (4).
- The composition of a refrigerant mix can be changed to improve the specific cooling power using these equations as guidelines.

References

[1] Radebaugh R. Cryocoolers: the state of the art and recent developments. J Phys: Condens Matter 2009;21:164219.

[2] Siegel PH. Terahertz technology. IEEE Trans Microw Theory Tech 2002;50(3):910.
[3] Yang CC, Nelson BL, Allen BR, Jones WL, Horton JB. Cryogenic characteristics of wide-band pseudomorphic HEMT MMIC low-noise amplifiers. IEEE Tans Microwave Theory Tech 1993;41:992.
[4] Mahdi AE, Mapps DJ. High-T SQUIDs: the ultra sensitive sensors for non-destructive testing and biomagnetism. Sens Actuators A: Phys 2000;81:367–70.
[5] Lewis RJ, Wang Y-D, Cooper J, Lin M-M, Bright VM, Lee YC, et al. Micro cryogenic coolers for ir imaging. Infrared technology and applications XXXVII. Proc. SPIE 2011.
[6] Venkatarathnam G. Cryogenic mixed refrigerant processes. In: Timmerhaus KD, Rizzuto Carlo, editors. The International Cryogenics Monograph Series. New York: Springer; 2008.
[7] Gong MQ, Deng Z, Wu J. Composition shift of a mixed-gas Joule–Thomson refrigerator driven by an oil-free compressor. Cryocoolers 2007;14:453–8.
[8] Narasimhan NL, Venkatarathnam G. A method for estimating the composition of the mixture to be charged to get the desired compassion in circulation in a single stage JT refrigerator operating with mixtures. Cryogenics 2010;50:93–101.
[9] Lewis RJ, Lin M-H, Wang Y, Cooper J, Bradley P, Radebaugh R, Huber M, Lee YC. Demonstration of a micro cryogenic cooler and miniature compressor for cooling to 200 K. In: Proceedings of the international mechanical engineering conference and exposition, Denver, Colorado, November; 2011. p. 63908.
[10] Lewis RJ, Wang Y-D, Lin M-H, Huber ML, Radebaugh R, Lee YC. Enthalpy change measurements of a mixed refrigerant in a micro cryogenic cooler in steady and pulsating flow regimes. Cryogenics 2012;52:609–14.
[11] Lerou PPPM, ter Brake HJM, et al. Insight into clogging of micromachined cryogenic coolers. Appl Phys Lett 2007;90:064102.
[12] Bonney GE, Longsworth RC. Considerations in using Joule-Thomson cryocoolers. In: Proceedings of the 6th International Cryocoolers Conference, vol. 1, Plymouth, Massachusetts, (October 25–26, 1990), David Taylor Research Center as DTRC-91/002, January 1991, p. 231–244.
[13] Maytal BZ, Pfotenhauer JM. "Transient Behavior", Miniature Joule–Thomson Cryocooling, 259–274. The international Cryogenics Monograph Series. New York: Springer; 2013.
[14] Burger JF, Holland HJ, Seppenwoolde JH, Berenschot E, ter Brake HJM, Gardeniers JGE, et al. Cryocoolers 2002;11:551–60.
[15] Lin M-H, Bradley PE, Huber ML, Lewis RJ, Radebaugh R, Lee YC. Mixed refrigerants for a glass capillary micro cryogenic cooler. Cryogenics 2010;50:439–42.
[16] Lin M-H, Bradley PE, Wu H-J, Booth JC, Radebaugh R, Lee YC. Design, fabrication, and assembly of a hollow-core fiber-based micro cryogenic cooler. In: Solid-State Sensors, Actuators and Microsystems Conference, 2009. TRANSDUCERS 2009. International Denver, Colorado, June 2009. p. 1114–7.
[17] Radebaugh R. Recent developments in cryocoolers. In: 19th Int. Congress of Refrigeration, 1995. p. 973–89.
[18] NIST Standard Reference Database 4. NIST Thermophysical Properties of Hydrocarbon Mixtures (SuperTrapp): Version 3.2, National Institute of Standards and Technology, Gaithersburg, MD; 2007.
[19] Lemmon EW, Huber ML, McLinden MO, NIST Standard Reference Database 23: Reference Fluid Thermodynamic and Transport Properties-REFPROP, Version 9.0, National Institute of Standards and Technology, Standard Reference Data Program, Gaithersburg; 2010.
[20] Lewis RJ, Yang YD, Bradley PE, Huber ML, Radebaugh R, Lee YC. Experimental investigation of low pressure refrigerant mixtures for micro cryogenic coolers. Cryogenics 2013.
[21] Bradley PE, Radebaugh R, Lewis RJ, Lin M-H, Lee YC, Temperature instability comparison of micro- and meso-scale Joule–Thomson cryocoolers employing mixed refrigerants. In: AIP Conference Proceedings (Proceedings of CEC/ICMC 2011), vol. 690, 2012. p. 1434.